Effect of synthesis method of LaNiO₃ type materials with perovskite structure on their features and in the methylene blue dye removal from aqueous media

Efeito do método de síntese de materiais de LaNiO₃ com estrutura perovskita nas suas características e na remoção do corante azul de metileno do meio aquoso

J. F. S. Ribeiro[1]; A. A. Souza[1], E. C. N. L. Lima[2]; M. J. B. Souza[3], A. M. Garrido Pedrosa[1,2*]

[1]Graduate Program in Chemistry / Federal University of Sergipe, 49100-000, São Cristóvão-SE, Brazil

[2]Department of Chemistry / Federal University of Sergipe, 49100-000, São Cristóvão-SE, Brazil

[3]Departament of Chemical Engenering / Federal University of Sergipe, 49100-000, São Cristóvão-SE, Brazil

*annemgp@ufs.br

Oxides with perovskite structure are the target of important studies, as they are versatile materials that have shown magnetic, electrical, optical, catalytic, adsorptive applications, among others, and are also easily synthesized. These applications are potentially influenced by the synthesis method, and in this sense, several methods have been used to prepare these materials, in order to optimize their characteristics and properties. The methods: modified protein using gelatin as a complexing agent, mechanosynthesis and combustion method in the heating plate and microwave were used to prepare LaNiO₃ type materials with perovskite structure used in the present work. The materials obtained were characterized by physical-chemical techniques (X-ray diffraction, nitrogen adsorption at 77 K and determination of the point of zero charge) and evaluated as an adsorbent for the removal of methylene blue dye in aqueous medium. All materials showed potential for removing the dye from the medium, with emphasis on the material obtained by mechanosynthesis, which presented higher methylene blue dye discoloration efficiency, due its smaller crystallite size and larger surface area. After the dye removal tests, the perovskite structure was preserved and the adsorbent was reused after being subjected to calcination at 900 °C for 2 hours when simultaneous degradation of the previously adsorbed dye occurred. The reused materials still had a high potential for dye removal.
Keywords: Perovskite, LaNiO₃, synthesis method

Óxidos com estrutura perovskita são alvo de importantes estudos, pois são materiais versáteis que apresentam aplicações magnéticas, elétricas, ópticas, catalíticas, adsortivas, entre outras, e também são facilmente sintetizados. Essas aplicações são potencialmente influenciadas pelo método de síntese e, nesse sentido, diversos métodos têm sido utilizados na preparação desses materiais, a fim de otimizar suas características e propriedades. Os métodos: proteíco modificada usando gelatina como agente complexante, mecanossíntese e método de combustão em placa de aquecimento e microondas foram usados para preparar os materiais do tipo LaNiO₃ com estrutura perovskita usadas no presente trabalho. Os materiais obtidos foram caracterizados por técnicas físico-químicas (difratometria de raios X, adsorção de nitrogênio a 77 K e determinação do ponto de carga zero) e avaliados como adsorventes para a remoção do corante azul de metileno em meio aquoso. Todos os materiais apresentaram potencial de remoção do corante do meio, com destaque para o material obtido por mecanossíntese, que apresentou maior eficiência de descoloração do corante azul de metileno, devido ao seu menor tamanho de cristalito e maior área de superfície. Após os testes de remoção do corante, a estrutura da perovskita foi preservada e o adsorvente foi reutilizado após ser submetido à calcinação a 900 °C por 2 horas quando ocorreu a degradação simultânea do corante previamente adsorvido. Os materiais reaproveitados ainda apresentavam alto potencial de remoção de corantes.
Palavras-chave: Perovskita, LaNiO₃, método de síntese

1. INTRODUCTION

Major industrial advances require the development of new technologies that provide lower cost and production optimization. Thus, it is necessary to search for new materials and methods that bring these characteristics to the processes carried out on a large scale. Currently, research is carried out to find production routes that mainly minimize costs as well as environmental impacts and optimize the efficiency of the materials obtained. In this scenario, studies on the synthesis methods of materials used as catalysts and/or adsorbents are of great relevance, as they provide the development of low cost techniques, with less damage to the environment and possibly more efficient materials [1-4].

Mixed oxides with perovskite structure, due in generally, they are reproducible synthesis materials and have high thermal and mechanical stability, have been the subject of studies for application in catalysis and adsorption [2, 4, 5]. Research shows that they are materials of potential applications in other areas, and therefore arouse interest in new ways of obtaining [6]. The main synthesis methods include the Pechini method, the chelating precursor method, the combustion method, sol-gel, co-precipitation and mechanic synthesis [2, 4-8].

The efficiency of materials with the perovskite structure for a particular application may be directly related to the synthesis method and the types of metals that form the ABX_3 type structure [7, 8]. One of the widely used perovskite synthesis methods is the ball milling process (mechanosynthesis), which can involve high energies allowing the occurrence of solid state reactions with formation of the perovskite phase through oxide mixtures without the need for the heat treatment step of the material at elevated temperatures. The heat treatment in muffle furnace is suggested as finishing, because it allows the diffusion of ions, forming the perovskite structure, through solid state reactions [7, 8].

A recent application that has been studied for mixed oxides with the perovskite structure is in the removal of liquid phase contaminants such as dyes [5]. This application is possible due the perovskite structure $LaMO_3$ (M = Ni, Mn, Co, Fe) they have ionic metallic sites that can interage with the dye structure, and due their stability there is the possibility of their recovery after application and re use. Dyes can cause serious problems ranging from the aesthetic nature of rivers and lakes to the loss of aquatic life [9]. Among the applied techniques for effluent treatment, adsorption has been employed to remove dyes [10].

As it is a spontaneous process, with low operating cost and high removal rates and with different possibilities [11-13], adsorption has been employed on an industrial scale. In addition, recovery of the adsorbent at the end of the procedure is almost 100% in most cases because it is a non-destructive method. Activated carbon is the most widely and efficiently used adsorbent. However, its high cost and difficult reuse are some of its disadvantages [14, 15]. In this context, the increasing and constant search for new adsorbent materials is justifiable. Other materials such as rice husk, sawdust, coconut shell, zeolites, clays, among others are also examples of materials that can be applied in adsorption with good efficiency in the removal of dyes in aqueous environment [16].

Methylene blue, being considered a model dye for the study of the removal of organic contaminants from aqueous solutions, is one of the most commonly used dyes in adsorption tests; It is used in the textile industry to dye cotton and wool fabrics [15-17]. It is a cationic dye of the phenothiazine class, which can cause various damages to human health, such as breathing difficulties due to its inhalation, diarrhea, vomiting, stomach pain and mental confusion due to its ingestion in high doses [18, 19].

The use of silica adsorbents such as silica, glass fibers and perlite for the removal of methylene blue dye in wastewater is increasing due to their high abundance, easy availability and low cost. Among these inorganic materials, amorphous silica deserves particular attention, considering the chemical reactivity of its hydrophilic sites, resulting from the presence of silanol groups, as well as its porous surface, high surface area and mechanical stability [20]. However, due to its low resistance to alkaline solutions the use is limited to a pH range lower than 8 [21].

In this context the present work aims to study the effect of $LaNiO_3$ type perovskite synthesis method on its structural and textural characteristics and on the removal of methylene blue dye in aqueous environment.

2. MATERIALS AND METHODS

2.1. Synthesis of materials

$LaNiO_3$ materials were synthesized by the synthesis methods described below with methodologies adapted from works proposed in the literature: modified protein method [22, 23], mechanosynthesis [24], plate combustion [25] and microwave [25]. All the synthesis procedures used in this work are described in more detail in Ribeiro's work [26].

For the synthesis of the material by the modified protein method, initially 1.2190 g of $Ni(NO_3)_2.6H_2O$ (Vetec, 97%) was dissolved in 100 mL of distilled water at 30 °C and kept under magnetic stirring for 5 minutes. Subsequently, 1.7657 g of $La(NO_3)_3.6H_2O$ (J.T. Baker, 99.9%) was added while stirring for a further 5 minutes at 30 °C. After this time the system was subjected to a temperature rise to stabilize at 70 °C, when 1.2191 g of gelatin (Royal) was added and kept under stirring for 1 hour. The obtained product was submitted to the pre calcination step with heating rate of 10 °C min^{-1} until reaching the temperature of 350 °C where it remained for 2 hours, forming the precursor powder. Part of the precursor powder was calcined at a heating rate of 10 °C min^{-1} until reaching 900 °C, remaining for 2 hours. The sample obtained was denominated LN-G9.

In the mechanosynthesis method, La_2O_3 (Vetec, 99.9%) and Ni_2O_3 (Vetec, 98%) were used as starting materials. The weight was weighed to obtain 2.5 g of final product. The heavy masses were added to the milling vessel, having a mass / powder ratio of 1:20. The vessel / beads / powder system was rotated at 400 rpm for 6 hours, so that every 2 hours of milling there was a 30 minutes break. At the end of 6 hours, part of the material was removed from the mill and stored. Another part was transferred to a porcelain crucible and immediately calcined at 10 °C min^{-1} until reaching 900 °C, remaining for 2 hours. The sample obtained was denominated LN-M9.

The synthesis of the material by the combustion method was performed in two steps in order to verify the influence of the heating source of the system (microwave or heating plate) in the material obtaining. For the synthesis of the material masses were weighed to obtain 2.0 g of final product. Initially, 2.4412 g of $Ni(NO_3)_2.6H_2O$ (Vetec, 97%) and 3.5267 g of $La(NO_3)_3.6H_2O$ (JT Baker, 99.9%) were solubilized in approximately 50 mL of distilled water under continuous stirring for 10 minutes at room temperature. At the same time, 2.0366 g of $CO(NH_2)_2$ (Vetec, 99%) were solubilized in 20 mL distilled water under continuous stirring at room temperature. Then the two solutions were mixed and homogenized for 5 minutes at room temperature on a stirring magnetic stirrer. The resulting solution contained in the beaker was placed on a heating plate at a temperature between 80 and 110 °C for partial evaporation of water to a volume of approximately 30 mL. After this step, which was performed in duplicate (for microwave and hotplate combustion), the final volume of the solution was placed for heating in a porcelain dish and on a hotplate where the temperature was raised to 300-350 °C until completion of combustion reaction. For microwave combustion, the solution was placed in a microwave apparatus where it was heated for about 10 minutes at a power of 70 W until the combustion reaction was completed. Then, part of the material obtained in both the microwave and hotplate combustion was stored and another part was calcined at a heating rate of 10 °C min^{-1} until reaching 900 °C, remaining for 2 hours. The materials obtained were denominated LN-CM9 and LN-CCH9, respectively.

2.2. Materials characterization

X-ray diffraction patterns were obtained using a Pananalytic diffractometer configured with Bragg geometry Radiation CuKα ($\lambda = 1.540562$ Å), 2θ in the range of 10 to 60° and scanning step of 5.0° min^{-1} were used. Peak identification was performed using JCPDS standard crystallographic forms. The data obtained from XRD analysis, besides allowing the identification of the phases present in the samples, allowed to calculate the average size of the crystallite through the Scherrer equation [24]. The crystallinity of the samples was determined from the methodology proposed in [26]. The total area values of the calcined samples at 900 °C were determined via nitrogen adsorption at 77 K in a NOVA 1200e Quantachrome equipment and using the BET method. The samples were previously degassed at 300 °C for 1 hour and then subjected to analysis. The pH of

the point of zero charge (pHpcz) for samples calcined at 900 ºC were determined using the batch method of equilibrium [26]. In a 50 mL beaker, 15 mg of each adsorbent to be analyzed and 20 mL of the previously prepared 0.10 mol L^{-1} NaCl solution were added, with pH values adjusted from 1 to 11 using NaOH or HCl 0 solutions at 10 mol L^{-1} and 0.05 mol L^{-1}. The mixtures were stirred at room temperature for one hour on a magnetic stirrer. After that, the samples were filtered on qualitative filter paper and the final pH of the solutions was measured with a bench pH meter (Micronal).

2.3. Dye removal tests

For the assays, aqueous solutions of the 10 mg L^{-1} methylene blue dye were prepared with pH measurement to make the medium basic and without pH measurement, which were diluted to 1 mg L^{-1} and analysed on the Shimadzu brand UV-Vis spectrophotometer and model UV-1800. Analysis were performed using 3.5 mL quartz cuvettes with 1.0 cm optical path and scanning at a wavelength range of 200 to 700 nm. In addition, the triplicate analytical curve of dye solutions at concentrations ranging from 0.5 to 3.0 mg L^{-1} ranging from 0.5 mg L^{-1} prepared from stock solution was also made. After obtaining the analytical curve and the dye absorption spectrum, studies were performed to evaluate the effects of contact time (using different adsorbents) and adsorbent mass on dye removal. All assays were conducted at room temperature of 25 °C and the perovskite used in the dye removal tests was previously dried at 60 °C for 30 minutes. Prior to the commencement of each dye discoloration assay, a suspension containing 100 mg of perovskite in 10 ml of 1 mol L^{-1} aqueous NaOH solution was prepared. This suspension was prepared by holding the mixture at room temperature (25 °C) and under magnetic stirring for 30 minutes. This suspension (perovskite / NaOH) was then added to 150 mL of the 10 mg L^{-1} dye solution and the system was subjected to magnetic stirring at room temperature (25 °C) to perform the dye removal assay. At established times (5, 30, 60, 90, 150, 180, 220, 280 and 360 minutes) aliquots of the supernatant were retired and centrifuged for 15 seconds at 2100 rpm rotation and analyzed on the spectrophotometer at the same conditions used in the reference solution with basic medium. The assays were conducted in triplicate, with a mean experiment error of 4% [26]. The effect of experimental conditions without the presence of adsorbent on dye degradation also studied. To study the effect of adsorbent mass, 50 mg, 75 mg and 100 mg of LaNiO$_3$ (LN-CCH9) adsorbent previously dried at 60 ºC for 30 minutes were used, following the methodology previously described for the study of contact time, but the UV-Vis spectrum was obtained only within 360 minutes. The efficiency (E%) and amount of adsorbed dye (q) in milligrams of dye per gram of adsorbent were estimated based on equations 01 and 02 [24].

$$E = \frac{100(C_0 - C_t)}{C_0} \tag{01}$$

Where C_t is the concentration of the solution at a given time and C_0 is the initial concentration of the solution.

$$q = \frac{V(C_0 - C_t)}{m} \tag{02}$$

Where: V is the volume of the solution, in L; C_0 is the initial concentration of the solution in mg L^{-1}; C_t is the concentration of the solution at time t in mg L^{-1}; m is the mass of the adsorbent in grams. The kinetic adsorption study was performed based on the pseudo-first-order [28], pseudo-second-order [29] and Elovich [30] models according to equations 03, 04 and 05, respectively, applying the experimental data.

$$q_t = q_1(1 - e^{(-k_1 t)}) \tag{03}$$

Where qt is the adsorption capacity at time t, in mg g^{-1}; q_1 is the theoretical value of equilibrium adsorption capacity in mg g^{-1}; k_1 is the pseudo-first order adsorption rate constant in min^{-1} and t is the time in min.

$$q_{t=} \frac{t}{\left(\frac{1}{k_2 q_2^2}\right) + \left(\frac{t}{q_2}\right)}$$
(04)

Where k_2 is the pseudo second order adsorption rate constant, in g mg^{-1} min^{-1}.

$$q_t = \frac{1}{\alpha} ln(1 + \alpha\beta t)$$
(05)

Where α (mg.g^{-1}.min^{-1}) is the initial adsorption rate and β (g^{-1}.min^{-1}) represents the desorption constant.

After the tests, the adsorbents were recovered and dried in an oven at 80 ºC for 1 hour and part of it was analyzed by X-ray diffractometry and another part was calcined at 900 ºC for 2 hours for dye degradation and adsorbent recovery. In the study of reuse of the LaNiO$_3$ material as adsorbent the same conditions described above were used, except that a single aliquot was collected in the time of 360 minutes and was analyzed similarly to the other samples in the first use.

3. RESULTS AND DISCUSSION

X-ray diffraction patterns of materials calcined at 900 °C showed the presence of the LaNiO$_3$ perovskite phase in all materials (Figure 1). For the material prepared by the modified protein method (LN-G9), the diffraction pattern revealed the presence of two high intensity peaks, related to the perovskite phase, whose 2θ angle are 32.83° and 47.34°, respectively and others of lower intensity also relating to perovskite structure such as 23.19°, 40.68°, 53.60° and 58.68°, all based on JCPDS card No.34-1028. According to JCPDS No.83-1355, the peak whose angle 2θ is 29.80° refers to La$_2$O$_3$. This product can be formed since lanthanum nitrate is one of the reagents used in the synthesis process [4, 6, 22-24]. For the material prepared by mechanosynthesis (LN-M9) it is possible to observe the presence of two peaks referring to the precursor powders, where one of them shows the La$_2$O$_3$ phase, according to the card JCPDS No.83-1355, whose angle 2θ is 37.31°, and 43.26° indicates the presence of NiO according to JCPDS card No.44-1159. Still for this material, there are the presence of peaks referring to the perovskite phase. Being two of the highest intensity, whose 2θ angles are 32.79° and 47.23°, and four low intensity peaks, whose 2θ angles are 23.16°, 40.56°, 53.56°, 58.55° based on JCPDS Letter No. 33-0711. From the diffraction pattern of the calcined material prepared by the microwave combustion method (LN-CM9), it is possible to perceive the presence of three higher intensity peaks referring to the perovskite phase, whose 2θ angles are 32.84°, 47.32° and 58.65°, and three other lower intensity peaks, whose angles 2θ are 23.20°, 40.74° and 53.62° based on JCPDS n° 34-1028. According to JCPDS No. 83-1355 and 44-1159, other phases are also present and refer to La$_2$O$_3$ and NiO, where the angles 2θ are 37.29° and 43.33°, respectively.
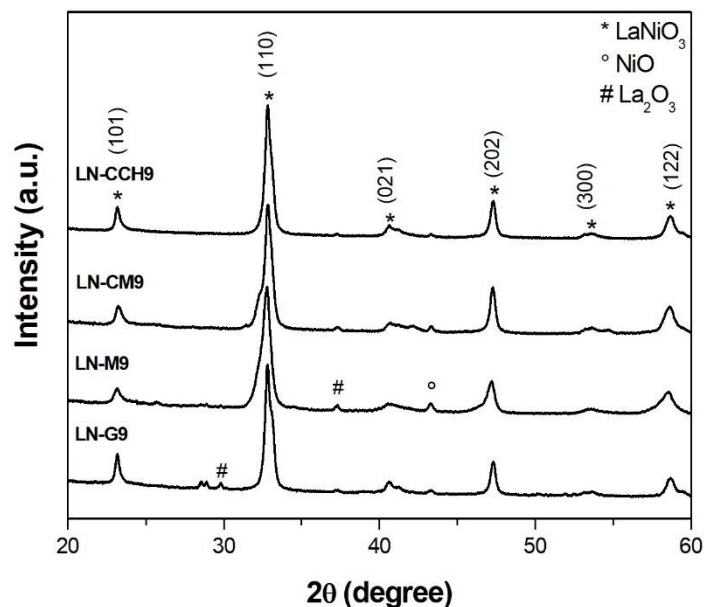
Figure 1. X-ray diffraction patterns of LaNiO₃ materials synthesized by different methods.

The diffraction pattern of the calcined material obtained by the plate combustion method (LN-CCH9) indicated the presence of high intensity peaks referring to the perovskite phase, whose 2θ angles are 23.20°, 32.85° and 47.34° and 58.67°, and low intensity peaks, but also referring to perovskite, whose 2θ angles are 40.64° and 53.59° based on JCPDS No. 34-1028. Measurement peak 2θ 43.36° refers to NiO according to JCPDS No.44-1159. As seen in diffraction patterns, the perovskite phase is the main one for all materials. However, other phases are present.

Table 1 shows the results for the average crystallite size for the $LaNiO_3$ phase synthesized by the different methods. The material synthesized by the modified protein method (LN-G9) presented a crystallite size of 17 nm, remaining consistent with previous studies, which obtained sizes between 11 and 15 nm for the $LaNiO_3$ phase synthesized by a similar method [23]. The results for the materials synthesized by the other methods presented smaller values of crystallite size in relation to the material synthesized by the modified protein method. For the material synthesized by the mechanosynthesis method (LN-M9), the smaller crystallite size was already expected as a result of the friction between the balls and the powders, causing fragmentation during the process [24]. The results also indicated that the sample prepared by plate combustion method had the biggest crystallinity, or degree of structural order due the peaks of $LaNiO_3$ phase are more intense. This sample was considered the standard sample. The crystallinity of the other samples refers to the structural order from them in relation to a standard sample (the most crystalline sample among all synthesized). The results shown in Table 1 indicate that the more heat involved in the synthesis step, the more crystalline the material.

Table 1. Crystallinity data and average crystallite size of LaNiO₃ material synthesized by different methods.

Synthesis method	Material	Average crystallite size (nm)	Crystallinity (%)
modified protein	LN-G9	17	69
mechanosynthesis	LN-M9	4	66
microwave combustion	LN-CM9	5	78
plate combustion	LN-CCH9	9	100

For a high adsorptive capacity in practical separation processes it is necessary to choose a suitable adsorbent. Adsorbents are typically porous solid particles, where their adsorption capacity is mainly measured by their textural properties [16]. One of the important characterizations for

adsorbent materials is the point of zero charge (PCZ). This parameter indicates the pH value at which a solid has zero charge on its surface. When the pH of the medium is lower than the PCZ pH of the material, its surface will be positively charged and adsorption of negatively charged particles (anionic species) will occur. Thus, when the pH of the medium is higher than the PCZ pH of the material, its surface will be negatively charged and adsorption of positively charged particles (cationic species) will occur [27]. As methylene blue is considered a cationic dye, its adsorption occurs when the pH of the medium is higher than the PCZ pH of the perovskite used in this work as adsorbent. Figure 2 shows the point of zero charge (PCZ) results for LaNiO$_3$ materials synthesized by different methods: LN-G9 (a), LN-CM9 (b), LN-CCH9 (c), and LN-M9 (d).
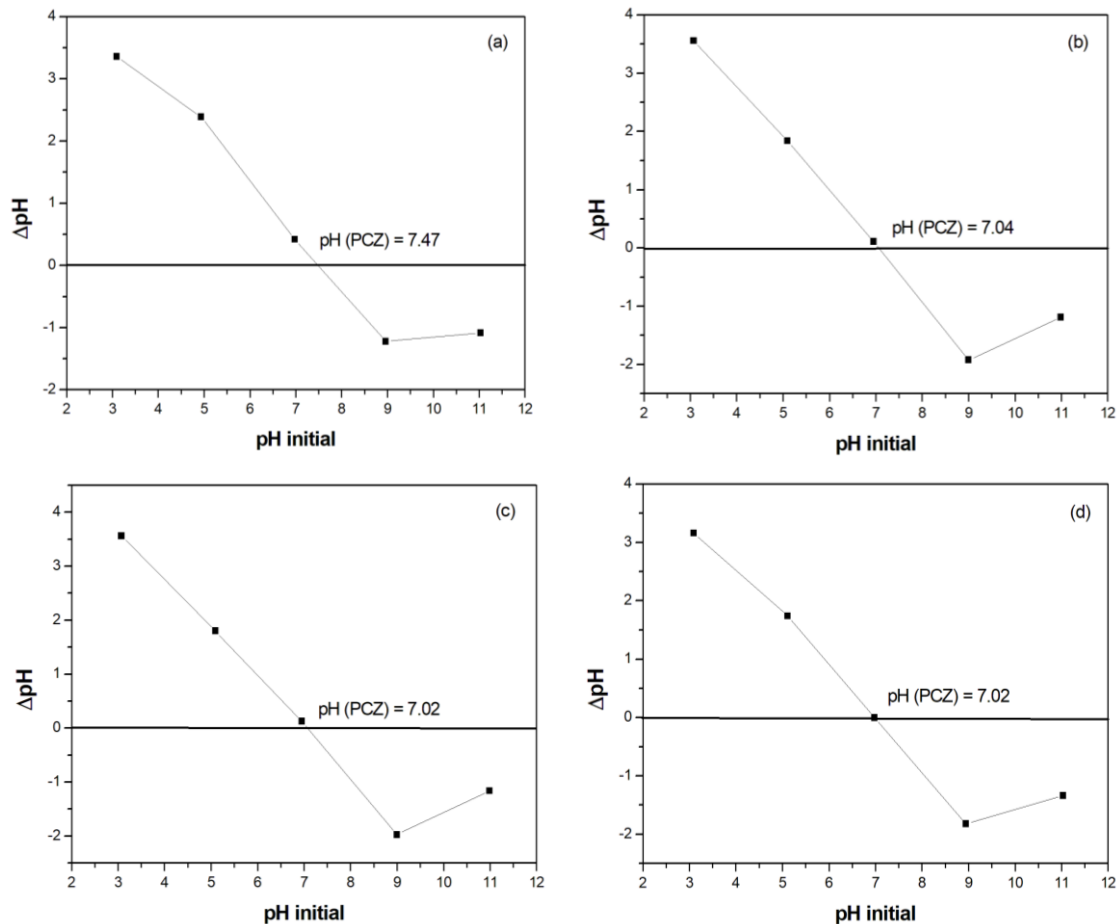

Figure 2. Point of zero charge (PCZ) for the materials LN-G9 (a), LN-CM9 (b), LN-CCH9 (c) and LN-M9 (d).

From the graphs in Figure 2, we can infer that the PCZ of LaNiO$_3$ type perovskite is approximately pH = 7 for all materials synthesized by the different synthesis methods. This value was already expected, since for the dye removal test at pH 4 the adsorption did not occur, while for the test at pH 9, the results revealed indications of a possible adsorption. However, the high adsorptive capacity of the material occurs at pH values greater than 9, where the surface of the material is more negatively charged interacting with cationic species such as methylene blue dye particles [27]. The surface area of adsorbents is also a relevant parameter for dye removal studies. The surface area of the LaNiO$_3$ perovskite synthesized by the different synthesis methods was determined by BET method [12]. Table 2 shows the results for the materials synthesized by the different synthesis methods. The area values for the materials synthesized by mechanosynthesis and combustion in the microwave were very close to the value reported in the literature, which is

26 m^2 g^{-1} for the same material synthesized by the modified protein method, but using the fiber soy instead of gelatin as a chelating agent [31].

Table 2. Total area (A$_{BET}$) and PCZ for the LaNiO$_3$ materials synthesized by different methods.

Synthesis method	Material	A$_{BET}$ (m g^{-1})	PCZ
modified protein	LN-G9	15 ± 1	7.47
mechanosynthesis	LN-M9	30 ± 2	7.02
microwave combustion	LN-CM9	25 ± 2	7.04
plate combustion	LN-CCH9	17 ± 1	7.02

Figure 3 shows the results of dye removal efficiency, E (%) and amount of dye adsorbed in milligrams per gram of adsorbent (q) in the mass study using LN-CCH9 material.
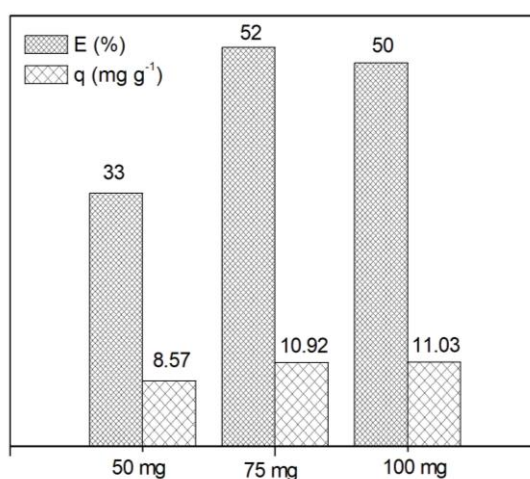

Figure 3. Efficiency of dye removal, E (%), and amount of dye removal (q) in the time of 360 minutes using LN-CCH9 material.

Through the data analysis, it can be inferred that for larger adsorbent masses, the removal efficiency happens more efficiently. It can still be observed that the efficiency and q values for the tests using the 75 and 100 mg masses occur quite similarly. The fact that the larger masses provide greater removal efficiency can be explained by the greater amount of adsorbent material in contact with the dye, enabling greater contact between the active sites responsible for the removal of methylene blue dye.

The kinetic study was performed applying the pseudo first order (PFO), pseudo second order (PSO) and Elovich models. Figures 4 show the graphs for these models, in addition to that Table 3 shows the parameters obtained and the correlation coefficients. According to the data of Figure 4 and Table 3, it is possible to verify that the experimental data of all dye adsorption assays using the different materials show a better fit to the Elovich kinetic model (R^2 near 1).

Table 3. Parameters obtained by the kinetic models of PFO, PSO and Elovich for adsorption of methylene blue dye using adsorbents LN-G9, LN-M9, LN-CM9 and LN-CCH9.

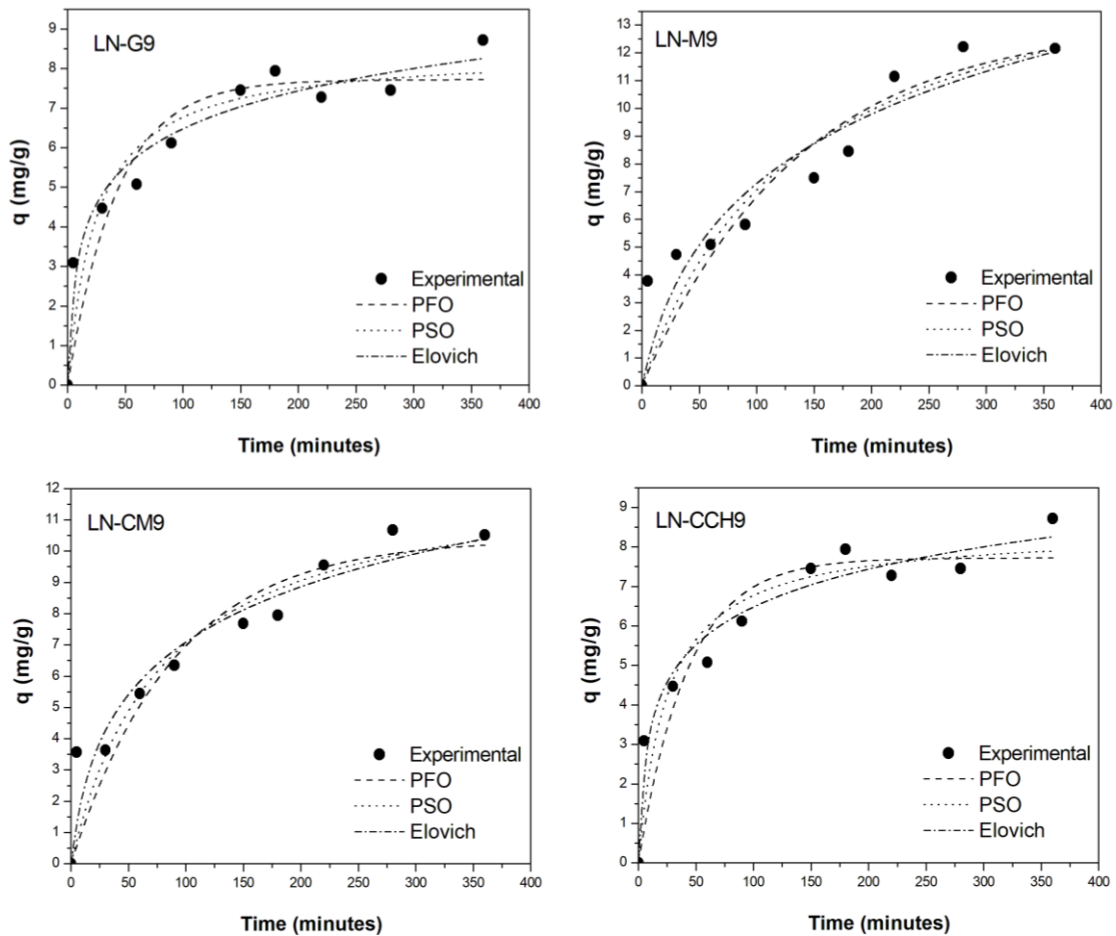|	Pseudo First Order		
Material	k_1 (min^{-1})	q_1 (mg g^{-1})	R^2
LN-M9	0.00735 ± 0.00272	13.08163 ± 2.1046	0.86043
LN-CM9	0.01234 ± 0.00353	10.37578 ± 0.98975	0.88734
LN-G9	0.04207 ± 0.01278	7.71811 ± 0.47628	0.88038
LN-CCH9	0.02357 ± 0.00648	7.71815 ± 0.47629	0.88038
	Pseudo Second Order		
Material	k_2 (g mg^{-1} min^{-1})	q_2 (mg g^{-1})	R^2
LN-M9	0.00043 ± 0.0003	16.79111 ± 3.47641	0.87277
LN-CM9	0.001 ± 0.00051	12.64933 ± 1.6025	0.90698
LN-G9	0.00483 ± 0.00205	8.43312 ± 0.58029	0.92129
LN-CCH9	0.00483 ± 0.00205	8.43316 ± 0.5803	0.92129
	Elovich		
Material	α (mg g^{-1} min^{-1})	β (g mg^{-1})	R^2
LN-M9	0.24165 ± 0.07363	0.19981 ± 0.09431	0.89019
LN-CM9	0.37146 ± 0.07765	0.34802 ± 0.16208	0.93015
LN-G9	0.71738 ± 0.08563	1.43962 ± 0.66886	0.96781
LN-CCH9	0.71738 ± 0.08563	1.43962 ± 0.66886	0.96781

Figure 4. Adsorption kinetics of methylene blue dye on materials LN-G9, LN-M9, LN-CM9 and LN-CCH9. Models: PFO = pseudo first order, PSO = pseudo second order and Elovich.

According to Elovich's model, α is the initial adsorption rate and β represents the desorption constant. It can be seen from the data in Table 3 that α values are low, indicating a low dye removal rate along the confirming a high amount of time for equilibrium to be achieved during testing as shown in Figure 4. The highest β values are for LN-G9 and LN-CCH9 materials, consequently lower dye removal efficiency due to the greatest desorption [32]. This fact can be explained according to the average crystallite size of the materials (Table 1). As for the LN-G9 and LN-CCH9 materials the highest average crystallite size values and for the LN-M9 and LN-CM9 materials, the smallest, therefore a larger contact surface, which allows a higher dye removal efficiency.

The adsorption efficiency of methylene blue (AM) using $LaNiO_3$ perovskites prepared by different methods is shown in Figure 05. It was observed that as a function of time, the dye removal efficiency, E (%), increases similar to observed by other papers [27].

Some important properties regarding the synthesis method can be analyzed to explain the results obtained for the dye removal efficiency, among them, the crystallite size, the BET area and the presence of secondary phases. As seen in Table 2, the average crystallite size for the materials synthesized by the mechanosynthesis and microwave combustion methods presented the lowest values, 4 and 5 nm, respectively. For materials synthesized by the plate combustion and modified protein methods, the values were 9 and 17 nm, respectively. This factor is relevance to dye removal efficiency. According to Figure 5, the material synthesized by mechanosynthesis presented higher removal efficiency (E), and this material was the one with the smallest crystallite size and the largest total area, and generally the smaller crystallite size results in the higher the removal efficiency [31].

The data shown in Table 2 also show that the material synthesized by mechanosynthesis presented a larger BET area, reinforcing the idea that the smaller the crystallite size, the larger the contact surface area and for this reason there is a higher removal efficiency for the material. The material synthesized by the modified protein method had the largest crystallite size and therefore the smallest surface area, resulting in a lower removal efficiency for this material compared to other materials. The other materials presented intermediate crystallite size and BET area and thus also intermediate removal efficiency. In addition, as previously shown by the diffraction pattern of Figure 01, the sample synthesized by mechanosynthesis presented more peaks due secondary phases than the materials synthesized by the other methods. Another fact observed was that up to 180 minutes the efficiency of materials in the removal of the dye from the medium grows gradually and similarly (Figure 5). However, after this time there is a significant difference in dye removal efficiency for different materials, which can possibly be explained from the idea that parameters such as crystallite size, surface area, number of secondary phases and the zero load point (PCZ) when summed are responsible for these differences in dye removal efficiencies and that these depend on the synthesis method [12, 31].
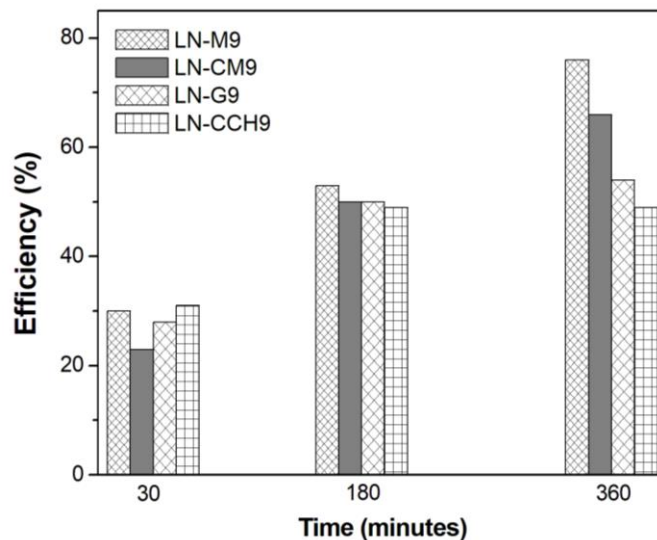

Figure 5. Dye removal efficiency at different times using LN-G9, LN-M9, LN-CM9 and LN-CCH9.

Verifying the integrity of materials after the tests is of great relevance, as it allows to verify if there is a possibility of recovery and reuse of perovskites in new adsorption tests. For this purpose, it is necessary to perform characterizations of the resulting system (perovskite/adsorbate). Figure 6 shows the X-ray diffraction patterns of $LaNiO_3$ material prepared by different synthesis methods after their uses in the removal tests. The results indicate that the perovskite peaks located at 2θ = 23.16°; 40.56°; 53.56°; 58.55°; according to JCPDS standard No. 33-0711 and 2θ = 23.19°; 32.83°; 40.68°; 47.34°; 53.60°; 58.68°; according to JCPDS standard No. 34-1028 remained present for all materials indicating that the $LaNiO_3$ perovskite with rhombohedral geometry was maintained as the main phase. In addition, the peak whose angle 2θ is 29.42° relative to La_2O_3 subtly increased its intensity for materials after first use.
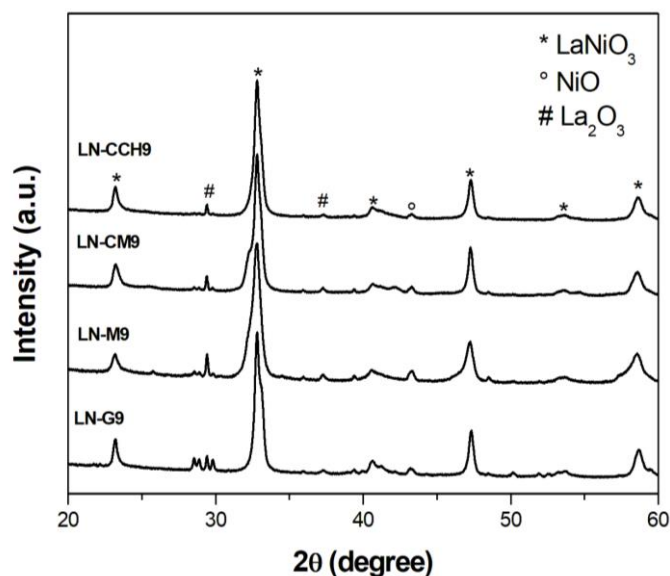

Figure 6. X-ray diffraction patterns of LaNiO₃-type materials synthesized by different methods used in dye removal tests.

According to the X-ray diffraction patterns of the materials used in the methylene blue dye removal tests in aqueous solution, the perovskite structure was maintained. In addition, the peaks have not been displaced. The facts corroborate a possible reuse of the material in new removal tests. Verifying the material's efficiency in reuse is of great relevance, and is a practice that has been performed in order to avoid discarding and waste. Some studies in the literature show that reused adsorbents can generally maintain their removal efficiency, such as potato peel used as methylene blue adsorbent in aqueous solution, where for the first use 35.83 mg.g^{-1} and 32.83 mg.g^{-1} for the second use [33]. Very close values, as well as for the materials used in the present work. Table 4 shows the dye removal efficiency data, E (%) and the amount (q) of dye adsorbed in mg per gram of adsorbent obtained in the first and reuse (second use) of materials LN-G9, LN-M9, LN-CM9 and LN-CCH9. For the second use the materials were calcined at 900 °C to remove organic phases from the adsorbed dye on the first use.

Table 4. Dye removal efficiency, E (%), and amount of dye (q) in time 360 minutes using LN-G9, LN-M9, LN-CM9 and LN-CCH9, for the first use (1st use) and second use (2st use) of the adsorbent.

Material	1st use		2st use	
	E (%)	q (mg/g)	E (%)	q (mg/g)
LN-M9	76	12.2	66	9.9
LN-CM9	66	10.5	62	9.2
LN-CCH9	49	7.9	45	6.7
LN-G9	54	9.0	59	8.9

From the data shown in Table 4, we can verify a close proximity in the removal efficiency values as well as in the q values as predicted by the X-ray diffraction patterns, because the perovskite structure remains after the first use. For all materials, in the second use, the efficiency occurred with a subtle decrease of values, except for the material synthesized by the modified protein method, which presented a higher efficiency value in the second use. However, the amount of dye removed from the medium is similar. Close values indicate that materials after calcination at 900 °C have similar effectiveness in removing methylene blue dye even after first use. This fact can be explained due to the great stability of the perovskite structure for $LaNiO_3$ material [6, 7]. In addition, calcination at this temperature was used for dye degradation.

Table 5 shows the amount of adsorbed methylene blue dye amount ($mg.g^{-1}$) for inorganic materials that present the oxide ion in their composition and the perovskite structure materials analyzed in the present work, demonstrating that the perovskite structure materials exhibit excellent removal efficiencies and can be considered promising adsorbents in the removal of methylene blue dye in aqueous medium. It is noteworthy that the experimental conditions for adsorption of methylene blue (AM) dye, using the different adsorbents, were different and that the purpose is to show other materials used for this purpose.

Table 5. Amount values of adsorbed methylene blue dye (q) for various materials.

Materials	q ($mg\ g^{-1}$)	Reference
Amorphous silica	22.66	[20]
Zeolite	10.82	[34]
LN-M9	12.2	Present work
LN-CM9	10.5	Present work
LN-G9	9.0	Present work
LN-CCH9	7.9	Present work

For the materials, the efficiency and amount of dye removed in both the first use and the second use increased when the largest BET area, the smallest average crystallite size, the smallest PCZ and the largest number of secondary phases.

4. CONCLUSIONS

$LaNiO_3$ type materials with perovskite structure can be obtained by the synthesis methods: modified protein, combustion, and mechanosynthesis. The presence of La_2O_3 and NiO secondary phases were identified in the material produced by the mechanosynthesis method. The secondary phase of the La_2O_3 type was found in the material produced by the modified protein method and the microwave combustion method. The NiO phase was found for the materials produced by the combustion method. The different synthesis methods used make it possible to obtain lanthanum nickelate with the perovskite structure, but with different types of secondary phases, average crystallite size, total area and load potential zero with small differences. All materials obtained showed potential to remove methylene blue dye from aqueous solutions in alkaline medium, which emphasizes the application of this material for this purpose. The $LaNiO_3$ material synthesized by the mechanosynthesis method presented a smaller crystallite size value, larger surface area, and a lower desorption value according to the Elovich kinetic model, corroborating a higher removal efficiency of the methylene blue dye for it. The perovskite structure is maintained after adsorption tests and all adsorbents can be reused after calcination, maintaining high efficiency values for removal of methylene blue dye from the aqueous environment.

5. ACKNOWLEDGEMENTS

6. BIBLIOGRAPHIC REFERENCES

1. Yahya N, Aziz F, Jamaludin NA, Mutalib MA, Ismail AF, Salleh WNW, Jaafar J, Yusof N, Ludin NA. A review of integrated photocatalyst adsorbents for wastewater treatment. J Environ Chem Eng. 2018;6:7411-7425, doi: 10.1016/j.jece.2018.06.051

2. Deka DJ, Gunduz S, Fitzgerald T, Miller JT, Co AC, Ozkan US. Production of syngas with controllable H_2/CO ratio by high temperature coelectrolysis of CO_2 and H_2O over Ni and Co- doped lanthanum strontium ferrite perovskite cathodes. Appl Catal. B. 2019;248:487-503, doi: 10.1016/j.apcatb.2019.02.045

3. Yang E. Moon DJ. Synthesis of $LaNiO_3$ perovskite using an EDTA cellulose method and comparison with the conventional Pechini method: application to steam CO_2 reforming of methane. RSC Advance 2016;6:112885-112898, doi: 10.1039/c6ra22945j

4. Moure C, Peña O. Recent advances in perovskites: Processing and properties. Prog Solid State Chem. 2015;43:123-148, doi: 10.1016/j.progsolidstchem.2015.09.001

5. Santos AG, Leite JO, Gimenez IF, Souza MJB, Garrido Pedrosa AM . Effect of the B-site cation from $LaBO_3$ and $LaBO_3/TiO_2$ (B = Mn or Ni) perovskites prepared by mechanosynthesis in adsorption of Congo red dye from aqueous medium. Mater Res Express. 2019;6:105065, doi: 10.1088/2053-1591/ab3b22

6. Fernandes, JDG, Melo, DMA, Ziner, LB, Salustiano, CM, Silva, ZR, Martinelli, AE, Cerqueira M, Alves Júnio C, Longo E, Bernardi MIB. Low-temperature synthesis of single-phase crystalline $LaNiO_3$ perovskite via Pechini method. Matter Lett. 2002;53:122-125, doi: 10.1016/s0167-577x(01)00528-6

7. Santos LPS, Siqueira JRR, Simoes A, Stojanovic BD, Paiva-Santos C O, Longo E, Varela JA. Influence of milling time on mechanically assisted synthesis of $Pb_{0,91}Ca_{0,1}TiO_3$ powders. Ceram Int. 2007;33:937-941, doi: 10.1016/j.ceramint.2006.02.004

8. Cristóbal AA, Botta PM, Bercoff PG, Porto López JM. Mechanosynthesis and magnetic properties of nanocrystalline $LaFeO_3$ using different iron oxides. Mater Res Bull. 2009;44:1036-1040, doi: 10.1016/j.materresbull.2008.11.015

9. Parida KM, Sahu S, Reddy KH, Sahoo PC. A Kinetic, Thermodynamic, and mechanistic approach toward adsorption of methylene blue over water-washed manganese nodule leached residues. Ind Eng Chem Res. 2010;50:843-848, doi: 10.1021/ie101866a

10. Kunz A, Peralta-Zamora P, Moraes SG, Durán N. Novas tendências no tratamento de efluentes têxteis. Quím Nova 2002;25:78-82, doi: 10.1590/s0100-40422002000100014

11. Liu X, Tian J, Li Y, Sun N, Mi S, Xie Y, Chen Z. Enhanced dyes adsorption from wastewater via Fe_3O_4 nanoparticles functionalized activated carbono. J Hazard Mater. 2019;373:397-407, doi: 10.1016/j.jhazmat.2019.03.103

12. Pavithra KG, Kumar PS, Jaikumar V, Rajan PS. Removal of colorants from wastewater: A review on sources and treatment strategies. J Ind Eng Chem. 2019;75:1-19, doi: 10.1016/j.jiec.2019.02.011

13. Allen SJ, Koumanova B. Decolourisation of water/wastewater using adsorption (review). J Univ Chem Technol Metallurgy. 2005;40:175-192, doi: 10.1016/j.cej.2009.04.063

14. Annadurai G, Juang RS, Lee DJ. Use of cellulose-based wastes for adsorption of dyes from aqueous solutions. J Hazard. Mater. 2002;92:263-274, doi: 10.1016/s0304-3894(02)00017-1

15. Aygun A, Yenisoy-Karakas S, Duman I. Production of granular activated carbon from fruit stones and nutshells and evaluation of their physical, chemical and adsorption properties. Microp Mesop Mat. 2003;66:189-195, doi: 10.1016/j.micromeso.2003.08.028

16. Yenisoy-Karakas S, Aygun A, Günes M, Tahtasakal E. Physical and chemical characteristics of polymer-based spherical activated carbon and its ability to adsorb organics. Carbon. 2004;42:477-484, doi: 10.1016/j.carbon.2003.11.019

17. Liu T, Li Y, Du Q, Sun J, Jiao Y, Yang G, Wang Z, Xia Y, Zhang W, Wang K, Zhu H, Wu D. Adsorption of methylene blue from aqueous solution by grapheme. Colloids Surf. B: Biointerfaces. 2012;90:197-203, doi: 10.1016/j.colsurfb.2011.10.019

18. Ghosh D, Bhattacharyya KG. Adsorption of methylene blue on kaolinite. Appl Clay Sci. 2002;20:295-300, doi: 10.1016/s0169-1317(01)00081-3

19. Karaca S, Gurscs A, Bayrak R. Effect of some pre-treatments on the adsorption of methylene blue by Balkaya lignite. Energy Convers Manag. 2004;45:1693-1704, doi: 10.1016/j.enconman.2003.09.026

20. Woolard C, Strong J, Erasmus C. Evaluation of the use of modified coal ashas a potential sorbent for organic waste streams. Appl Geochem. 2002;17:1159-1164, doi: 10.1016/s0883-2927(02)00057-4

21. Ahmed MN, Ram RN. Removal of basic dye from wastewater using silica as adsorbent. Environ Pollut. 1992;77:79-86, doi: 10.1016/0269-7491(92)90161-3

22. Santos JC, Souza MJB, Ruiz JAC, Melo DMA, Mesquita ME, Garrido Pedrosa AM. Synthesis of LaNiO$_3$ perovskite by the modified proteic gel method and study of catalytic properties in the syngas production. J Braz Che. Soc. 2012;23:1858-1862, doi: 10.1590/s0103-50532012005000052

23. Moraes Júnior EO, Leite JO, Santos AG, Souza MJB, Garrido Pedrosa AM. Nickel-based perovskite catalysts: synthesis and catalytic tests in the production of syngas. Cerâmica. 2018;64:436-442, doi: 10.1590/0366-69132018643712329

24. Santos AG, Leite JO, Souza MJB, Gimenez IF, Garrido Pedrosa, AM. Effect of the metal type in perovskites prepared by modified proteic method in dye adsorption from aqueous médium. Ceram Int. 2018;44:5743-5750, doi: 10.1016/j.ceramint.2017.12.232

25. Costa ACFM, Tortella E, Morelli MR, Kiminami RHGA. Nanosize Ni0.7Zn0.3Fe2O4 Powders prepared by combustion synthesis, sintering and characterization. J. Meta stable Nanocryst Mater. 2002;14:57-64, doi: 10.4028/www.scientific.net/jmnm.14.57

26. Ribeiro JFS. Estudo do método de síntese de materiais com estrutura perovskita nas características estruturais e na remoção do corante azul de metileno [master's dissertation]. São Cristóvão (SE): Universidade Federal de Sergipe; 2019. 72 p.

27. Giacomni F, Menegazzo MAB, Silva MG, Silva AB,Barros MASD. Importância da determinação do ponto de carga zero como característica de tingimento de fibras proteicas. Matéria. 2017;22(2):e11827, doi: 10.1590/s1517-707620170002.0159

28. Lopes ECN, dos Anjos FSC, Vieira EFS, Cestari AR. An alternative Avrami equation to evaluate kinetic parameters of the interaction of Hg(II) with thin chitosan membranes. J Colloid Interf Sci. 2003;263:542-547, doi: 10.1016/s0021-9797(03)00326-6

29. Matos TTS, de Jesus, AMD, Araújo BR, Romão LPC, Santos LO, Santos J M. Aplicação de subprodutos industriais na remoção de corantes reativos têxteis. Rev Virtual Quím. 2013;5:840-853, doi: 10.5935/1984-6835.20130061

30. Qiu H, Lv L, Pan BC, Zhang QJ, Zhang W, Zhang Q. Critical review in adsorption kinetic models. J Zhejiang Univ Sci. A. 2009;10:716-724, doi: 10.1631/jzus.A0820524

31. Bradha M, Vijayaraghavan T, Suriyaraj SP, Selvakumar R, Ashok AM. Synthesis of photocatalytic La$_{(1-x)}$A$_x$TiO$_{3.5-\delta}$ (A=Ba, Sr, Ca) nano perovskites and their application for photocatalytic oxidation of congo red dye in aqueous solution. J Rare Earths 2015;33:160-167, doi: 10.1016/S1002-0721(14)60397-5

32. Silva JE, Rodrigues FIL, Pacífico SN, Santiago LF, Muniz C, Saraiva GD, Nascimento RF, Sousa Neto VO. Estudo de cinética e equilíbrio de adsorção empregando a casca do coco modificada quimicamente para a remoção de Pb(II) de banho sintético. Rev Virtual Quím. 2018;10:1248-1263, doi: 10.21577/1984-6835.20180086

33. Alfredo APC, Gonçalves GC, Lobo VS, Montanher SF. Adsorção de azul de metileno em casca de batata utilizando sistemas em batelada e coluna de leito fixo. Rev Virtual Quím. 2015;7:1909-1920, doi: 10.5935/1984-6835.20150112

34. Dogan M, Alkan M, Onager Y. Adsorption of methylene blue from aqueous solution onto perlite. Water Air Soil Pollut. 2000;120:229-248, doi: 10.1023/A:1005297724304